

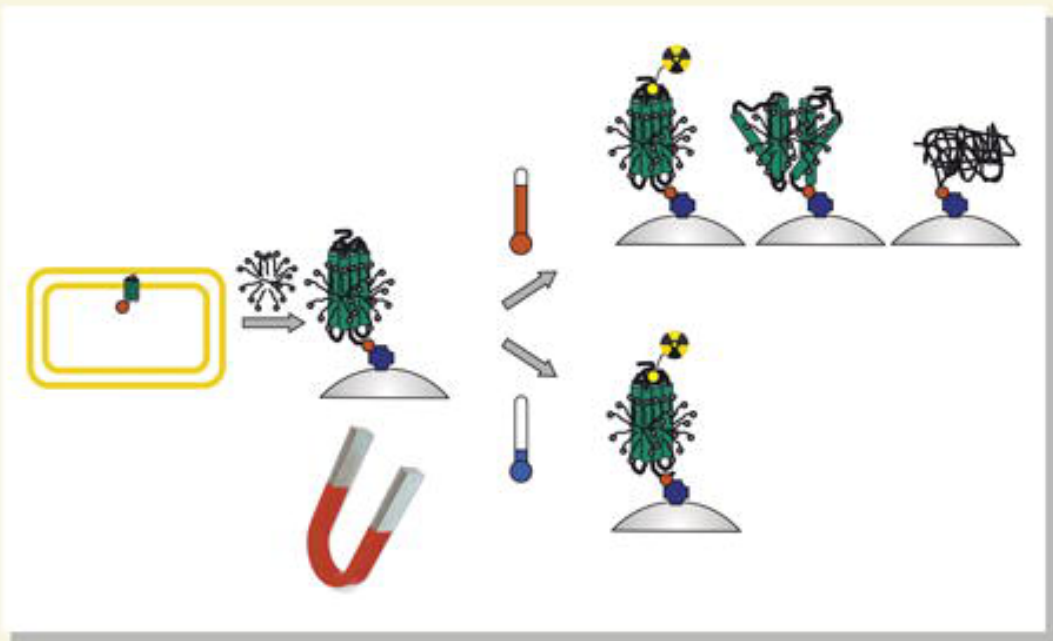


Volume 408, Issue 4, 13 May 2011

ISSN 0022-2836

# JMB

JOURNAL OF MOLECULAR BIOLOGY



0022-2836(20110513)408:4;1-Y



## COMMENTARY

## New Tools for Breaking Barriers to GPCR Expression in *E. coli*

In this *Journal of Molecular Biology* issue, Plückthun *et al.* describe the use of directed evolution and fluorescence-activated cell sorting-based screening to select for high-level expression of a historically challenging class of membrane protein targets, G protein-coupled receptors. Membrane proteins, particularly from eukaryotic sources, have historically been difficult to produce in *Escherichia coli*, which has limited the ability to use this inexpensive host to produce protein for biochemical and structural studies, including metabolically labeled protein for NMR studies (reviewed in Refs. 1–3). In recent years, more eukaryotic membrane proteins have been crystallized, but the majority of these have been produced in yeast or insect cells.<sup>4</sup> Membrane protein expression in bacteria typically results in inclusion body formation, resulting in protein that can be difficult to denature and refold, or in degradation, with low yields of correctly folded, membrane-inserted protein.<sup>5</sup> Recently, several groups have developed genetic or rational approaches to developing engineered strains to improve membrane protein expression in *E. coli*, which have resulted in relatively modest increases in protein expression that are protein dependent.<sup>6–8</sup> These increases have been observed both for proteins that have low expression and for proteins previously shown to have little to no expression in prokaryotic systems.<sup>6–8</sup>

The work of Plückthun *et al.* takes these approaches to a new level. In 2008, they developed an alternate strategy to improve the expression of membrane proteins in *E. coli* using directed evolution of the protein sequence and showed the feasibility of this approach for G protein-coupled receptor expression using the rat neurotensin-1 receptor.<sup>9</sup> Their engineered variant, neurotensin-1-D03, was expressed at ~6-fold higher levels than wild-type protein (ca 700 receptors/cell), with wild-type ligand-binding properties. In the current work, Dodevski and Plückthun has focused on a particularly intransigent target, the neurokinin 1 receptor, which has been shown to be poorly expressed in

many expression systems,<sup>10,11</sup> can only produce ~200 soluble receptors/cell in *E. coli* and, although it can form inclusion bodies, has been recalcitrant to refolding strategies.<sup>12</sup> In addition, Dodevski and Plückthun show the widespread applicability of this approach to other receptors with diverging expression levels—the adrenergic  $\alpha_{1a}$  and  $\alpha_{1b}$  receptors, which are natively expressed at ~350 and 2000 copies/cell, respectively.<sup>10</sup> In all cases, the evolved receptors expressed at ~3000 copies/cell (~1 mg/L at an OD<sub>600</sub> of 0.5), independent of initial expression levels, suggesting a potential membrane capacity limitation for this prokaryotic cell.

The paper also describes an interesting high-throughput screening approach for receptor solubility based on *in vivo* biotinylation of the receptors with native BirA, followed by streptavidin/magnetic bead separation. The magnetic isolation is readily applied in a 96-well format, enabling a rapid screen under different detergent or solution conditions.<sup>10</sup> The authors demonstrate the robustness of this technique to employ a stability screen of 200–300 evolved variants, ultimately identifying receptors with both higher expression levels and higher stability compared to wild-type parents. One caveat to the evolution approach is that screening is based on binding to one agonist, and affinity to other ligands or coupling to G proteins may be altered. Despite this potential limitation, this directed evolution and stability screen approach provide an exciting addition to the growing toolbox for those interested in prokaryotic expression of membrane proteins for biochemical, biophysical and structural characterization.

### References

1. White, S. H. (2004). The progress of membrane protein structure determination. *Protein Sci.* **13**, 1948–1949.
2. Tate, C. G. (2001). Overexpression of mammalian integral membrane proteins for structural studies. *FEBS Lett.* **504**, 94–98.

3. Chiu, M. L., Tsang, C., Grihalde, N. & MacWilliams, M. P. (2008). Over-expression, solubilization, and purification of G protein-coupled receptors for structural biology. *Comb. Chem. High Throughput Screening*, **11**, 439–462.
4. Robinson, A. S. & Loll, P. J. (2011). Introduction: current challenges in membrane protein production. In *Production of Membrane Proteins: Strategies for Expression and Isolation* (Robinson, A. S., ed.), pp. 424, Wiley-VCH, Weinheim, Germany.
5. Link, A. J. & Georgiou, G. (2007). Advances and challenges in membrane protein expression. *AIChE. J.* **53**, 752–756.
6. Skretas, G. & Georgiou, G. (2010). Simple genetic selection protocol for isolation of overexpressed genes that enhance accumulation of membrane-integrated human G protein-coupled receptors in *Escherichia coli*. *Appl. Environ. Microbiol.* **76**, 5852–5859.
7. Wagner, S., Klepsch, M. M., Schlegel, S., Appel, A., Draheim, R., Tarry, M. *et al.* (2008). Tuning *Escherichia coli* for membrane protein overexpression. *Proc. Natl Acad. Sci. USA*, **105**, 14371–14376.
8. Massey-Gendel, E., Zhao, A., Boulting, G., Kim, H. Y., Balamotis, M. A., Seligman, L. M. *et al.* (2009). Genetic selection system for improving recombinant membrane protein expression in *E. coli*. *Protein Sci.* **18**, 372–383.
9. Sarkar, C. A., Dodevski, I., Kenig, M., Dudli, S., Mohr, A., Hermans, E. & Plückthun, A. (2008). Directed evolution of a G protein-coupled receptor for expression, stability, and binding selectivity. *Proc. Natl Acad. Sci. USA*, **105**, 14808–14813.
10. Dodevski, I. & Plückthun, A. (2011). Evolution of three human GPCRs for higher expression and stability. *J. Mol. Biol.* **408**, 599–615.
11. Lundstrom, K., Wagner, R., Reinhart, C., Desmyter, A., Cherouati, N., Magnin, T. *et al.* (2006). Structural genomics on membrane proteins: comparison of more than 100 GPCRs in 3 expression systems. *J. Struct. Funct. Genomics*, **7**, 77–91.
12. Bane, S. E., Velasquez, J. E. & Robinson, A. S. (2007). Expression and purification of milligram levels of inactive G-protein coupled receptors in *E. coli*. *Protein Expression Purif.* **52**, 348–355.

Anne Robinson  
University of Delaware,  
Newark, DE 19716, USA  
E-mail address: [asr@udel.edu](mailto:asr@udel.edu).



# Evolution of Three Human GPCRs for Higher Expression and Stability

Igor Dodevski and Andreas Plückthun\*

Department of Biochemistry, University of Zurich, Winterthurerstrasse 190, CH-8057 Zurich, Switzerland

Received 21 December 2010;  
received in revised form  
21 February 2011;  
accepted 22 February 2011  
Available online  
3 March 2011

Edited by J. Bowie

## Keywords:

GPCR;  
directed evolution;  
stability;  
protein engineering;  
expression in *E. coli*

We recently developed a display method for the directed evolution of integral membrane proteins in the inner membrane of *Escherichia coli* for higher expression and stability. For the neurotensin receptor 1, a G-protein-coupled receptor (GPCR), we had evolved a mutant with a 10-fold increase in functional expression that largely retains wild-type binding and signaling properties and shows higher stability in detergent-solubilized form. We have now evolved three additional human GPCRs. Unmodified wild-type receptor cDNA was subjected to successive cycles of mutagenesis and fluorescence-activated cell sorting, and functional expression could be increased for all three GPCR targets. We also present a new stability screening method in a 96-well assay format to quickly identify evolved receptors showing increased thermal stability in detergent-solubilized form and rapidly evaluate them quantitatively. Combining the two methods turned out to be very powerful; even for the most challenging GPCR target—the tachykinin receptor NK<sub>1</sub>, which is hardly expressed in *E. coli* and cannot be functionally solubilized—receptor mutants that are functionally expressed at 1 mg/l levels in *E. coli* and are stable in detergent solution could be quickly evolved. The improvements result from cumulative small changes in the receptor sequence. This combinatorial approach does not require preconceived notions for designing mutations. Our results suggest that this method is generally applicable to GPCRs. Existing roadblocks in structural and biophysical studies can now be removed by providing sufficient quantities of correctly folded and stable receptor protein.

© 2011 Elsevier Ltd. All rights reserved.

\*Corresponding author. E-mail address:  
[plueckthun@bioc.uzh.ch](mailto:plueckthun@bioc.uzh.ch).

Present address: I. Dodevski, Johnson Research Foundation and Department of Biochemistry and Biophysics, University of Pennsylvania, Philadelphia, PA 19104-6059, USA.

Abbreviations used: GPCR, G-protein-coupled receptor; FACS, fluorescence-activated cell sorting; NTR1, neurotensin receptor 1; wt, wild type;  $\alpha_{1a}$ AR,  $\alpha_{1a}$  adrenergic receptor;  $\alpha_{1b}$ AR,  $\alpha_{1b}$  adrenergic receptor; PBS, phosphate-buffered saline; MFI, mean fluorescence intensity; LBA, ligand binding assay; DDM, dodecyl- $\beta$ -D-maltopyranoside; CHAPS, 3-[(3-cholamidopropyl)dimethylammonio]propanesulfonic acid; CHS, cholesteryl hemisuccinate; SI, stability index; BSA, bovine serum albumin; EDTA, ethylenediaminetetraacetic acid; LBB, ligand binding buffer; TKCl, Tris-HCl/KCl; TM, transmembrane.

## Introduction

G-protein-coupled receptors (GPCRs) represent the largest superfamily of cell surface receptors in the living world. They respond to an enormous diversity of extracellular signals, including neurotransmitters, hormones, ions, and photons. When an incoming signal activates a GPCR, the receptor undergoes large conformational rearrangements whereby the signal is transmitted to intracellular effector proteins. This mechanism allows for the activation of a variety of different intracellular signaling pathways.

Because of the enormous diversity in received signals, GPCR signaling is involved in nearly every physiological process, and deregulated signaling readily leads to pathological conditions. Of the

nearly 800 different GPCRs identified in the human genome,<sup>1</sup> about 300 GPCRs are considered pharmaceutically relevant (not counting the receptors for odor or taste). Presently, about 30 of these are targeted by about 25% of all known drugs in clinical use.<sup>2,3</sup> The remaining majority of GPCRs are considered potential high-value drug targets. Due to the central biomedical role of GPCRs in human physiology and pathology, they are being very actively researched in both academia and industry.

Among these research efforts, the crystallographic determination of a three-dimensional receptor structure represents a central methodology for investigating GPCR function at atomic resolution. Despite tremendous research efforts made in GPCR crystallography, structure determination has remained enormously difficult because of the properties of the protein, and to date, the structures of only six different GPCRs could be solved.<sup>4–10</sup> Moreover, this set is somewhat redundant because the  $\beta_1$  and  $\beta_2$  adrenergic receptors are very closely related, and the visual cone pigment rhodopsin was solved from two different species. Yet, the structures provide detailed structural insights into receptor function and ligand binding contacts at atomic resolution, and they were successfully used for structure-based ligand discovery.<sup>11</sup> Analysis of the six receptor structures reveals many conserved structural features as well as many important structural differences that may account for the enormous functional diversity observed in GPCR signaling. It is very likely that the important and often unique structural differences cannot be extrapolated between different members of the GPCR superfamily by molecular modeling. It will therefore be necessary to solve the structure of most GPCRs individually to fully explore their pharmacological potential and to understand the mechanism of action of agonists or antagonists from the structural biology point of view.

The experimental procedure of obtaining a crystal structure typically involves three steps: the protein has to be functionally expressed, purified in detergent micelles, and crystallized. However, for most integral membrane proteins, especially for those of animal origin such as GPCRs, each of these steps turns out to be very problematic. GPCR expression in native tissue is typically very low, and it is therefore necessary to set up a robust recombinant expression system. Standard techniques for finding acceptable overexpression conditions include screening of expression hosts, promoters, fusion adducts, and protein homologs. However, even if all of these expression parameters are optimized, most GPCRs may not yield sufficient material for crystallographic studies. When acceptable expression conditions are found, the problem of extracting the GPCR out of the lipid bilayer by detergents limits the process toward crystallization because most

GPCRs are intrinsically unstable proteins and quickly lose their native fold when solubilized.

In a previous study, we addressed these roadblocks by analyzing the capacity of the receptor sequence itself as an experimental parameter for overcoming the problems of low receptor expression and marginal stability.<sup>12</sup> To this end, we had developed a directed evolution method consisting of random mutagenesis and selection by fluorescence-activated cell sorting (FACS). By applying this evolutionary selection method to the model GPCR neurotensin receptor 1 (NTR1), we had identified mutations that strongly improve functional surface expression and stability, while wild-type (wt) biochemical function was largely retained.<sup>12</sup> In the present study, we further validate this directed evolution method on three additional human GPCRs of the rhodopsin family.

More specifically, we wanted to characterize two important technical aspects of the method in order to assess its potential for being generally applicable to other members of the GPCR superfamily. The first aspect relates to the possibility of increasing functional expression, independent of whether the wt expression level is already at least moderate, by evolving even very weakly expressed GPCRs. The second aspect relates to the identification of stabilized receptor mutants in a pool of well-expressed mutants by a newly developed stability screen in a 96-well assay format. We investigated the performance of the new stability screen to see how readily stable receptor mutants can be identified among the well-expressed ones. The new stability screen turned out to be very powerful for isolating stabilized receptor mutants, which can be functionally solubilized, starting from a wt receptor that cannot be functionally solubilized to any measurable degree.

## Results

### Selection method for increasing functional expression and stability of three human GPCRs

To evaluate the performance of our selection method for evolving both increased functional expression levels and receptor stability of GPCRs, we chose three different human GPCRs of the rhodopsin family. With the use of the same expression system with which the wt rat NTR1 receptor gave ca 700 receptors/cell,<sup>12,13</sup> the wt cDNA of the receptors tested here showed different functional expression levels in *Escherichia coli*. The tachykinin receptor NK<sub>1</sub> expressed ~100–300 receptors/cell, the  $\alpha_{1a}$  adrenergic receptor ( $\alpha_{1a}$ AR) expressed ~350 receptors/cell, and the  $\alpha_{1b}$  adrenergic receptor ( $\alpha_{1b}$ AR) expressed ~2000 receptors/



cell. The wt receptors also show distinctive behavior when solubilized in detergent micelles. While the two  $\alpha$  adrenergic receptor subtypes ( $\alpha_{1a}$ AR and  $\alpha_{1b}$ AR) show functional radioligand binding when solubilized in detergent micelles, the tachykinin receptor NK<sub>1</sub> lacks sufficient stability to do so. These differences in expression and stability make the receptors excellent targets for characterizing the performance of our selection method for increasing receptor expression and stability. It extends our previous work to receptors expressing at much lower levels and with much lower stability than rat NTR1.<sup>12</sup> Clearly, the very poor biophysical properties of NK<sub>1</sub> make it the most challenging target.

The implementation of the selection method for the three receptors was facilitated by the commercial availability of high-affinity fluorescent ligands. These ligands are required for evolving functional receptor by the FACS-based selection method. NK<sub>1</sub> is a peptide-binding receptor, and it binds to the 11-amino-acid-long peptide Substance P, which acts as an endogenous high-affinity agonist to NK<sub>1</sub>. For the NK<sub>1</sub> selections, Substance P was used as an Oregon Green derivative (SP-OG). The adrenergic receptors  $\alpha_{1a}$ AR and  $\alpha_{1b}$ AR belong to the amine binding class of GPCRs, and they bind with high affinity to the small-molecule antagonist prazosin. For the selections of these receptors, prazosin was used as a BODIPY-FL derivative (prazosin-BFL) (see [Materials and Methods](#)).

For FACS-based selections, specific binding of fluorescent ligand to the receptor serves as an indicator for functionally expressed receptor inserted in the inner plasma membrane of the expression host *E. coli*.<sup>12</sup> In order to bind to the receptors located in the inner membrane, the fluorescent ligands must be able to partition across the outer membrane of *E. coli*. A suitable binding buffer must therefore be formulated such that the outer membrane becomes permeable without compromising cell viability. Furthermore, the binding buffer should not contain any components that inhibit ligand binding to the receptor. For NK<sub>1</sub>, we used a modified 5-fold concentrated phosphate-buffered saline (PBS) buffer (5×PBS-K) (see [Materials and Methods](#)), which we adapted from the work published by Chen *et al.*<sup>14</sup> The modification consisted of substituting potassium for sodium in PBS to avoid the inhibitory effect that sodium ions may have on SP-OG binding.<sup>15</sup> For  $\alpha_{1a}$ AR and  $\alpha_{1b}$ AR, we used a buffer containing 50 mM Tris-HCl and 100 mM KCl [Tris-HCl/KCl (TKCl)] (see [Materials and Methods](#)).

### Evolving receptors for higher functional expression

The general selection method for evolving higher expression levels of GPCRs by FACS has been

described in our previous paper.<sup>12</sup> In the present study, we applied the selection method to three additional receptors, namely, NK<sub>1</sub>,  $\alpha_{1a}$ AR, and  $\alpha_{1b}$ AR. During the process of receptor evolution, the functional expression level of the evolving receptor pools increased for each of the receptors with each round of mutagenesis and selection, as evidenced by an increase in the specific mean fluorescence intensity (MFI). [Figure 1](#) shows the increase in MFI after two rounds of evolution (ep2 pool) and four rounds of evolution (ep4 pool) for the three receptor targets. In our strategy, one round of evolution consists of one step of error-prone PCR (hence the letters “ep” in the nomenclature of the evolved receptor pools) and four to six rounds of sorting for the most fluorescent cells by FACS (e.g., the receptors in the ep4 pools have been evolved for four rounds).

The evolution of NK<sub>1</sub> started from a wt cDNA that is expressed so weakly that specific ligand binding can hardly be measured by FACS, as indicated by the histograms of total and nonspecific MFI that are almost overlapping for wt NK<sub>1</sub> ([Fig. 1](#)). After four rounds of evolution, the specific MFI of the selected NK<sub>1</sub> clones (ep4 pool) was approximately five times higher than that of the wt receptor. Similarly, the evolution of  $\alpha_{1a}$ AR started from a relatively weakly expressed wt receptor cDNA ([Fig. 1](#)). After four rounds of evolution, the specific MFI of the selected  $\alpha_{1a}$ AR clones (ep4 pool) was also approximately five times higher than that of the wt receptor. In contrast to wt NK<sub>1</sub> and wt  $\alpha_{1a}$ AR, which were very weakly expressed, wt  $\alpha_{1b}$ AR was expressed relatively well (i.e., approximately fivefold better than its close homolog  $\alpha_{1a}$ AR). We evolved  $\alpha_{1b}$ AR for two rounds, and the selected ep2 pool reached a specific MFI two times higher than that of the wt receptor ([Fig. 1](#)).

To quantitatively assess the increase in functional expression of single evolved receptors in the pools, we performed radioligand binding assays [ligand binding assays (LBAs)] on whole *E. coli* cells of randomly picked single clones. We used constant radioligand concentrations (10 nM) that are 5- to 10-fold above the  $K_d$  of the wt receptors.

### Expression level of evolved NK<sub>1</sub> receptors

Using the same expression system as described previously for NTR1,<sup>12,13</sup> we observed a very weak expression of the wt cDNA of NK<sub>1</sub> in *E. coli* at a level of only 100–300 receptors/cell. In total, we applied four rounds of evolution to NK<sub>1</sub>. After two rounds of evolution (ep2 pool), we isolated single receptor variants that expressed up to 1200 receptors/cell ([Supplementary Fig. 1a](#)). Two additional rounds of evolution augmented the expression level further, and the best receptor variants in the ep4 pool expressed more than 2000 receptors/cell, which

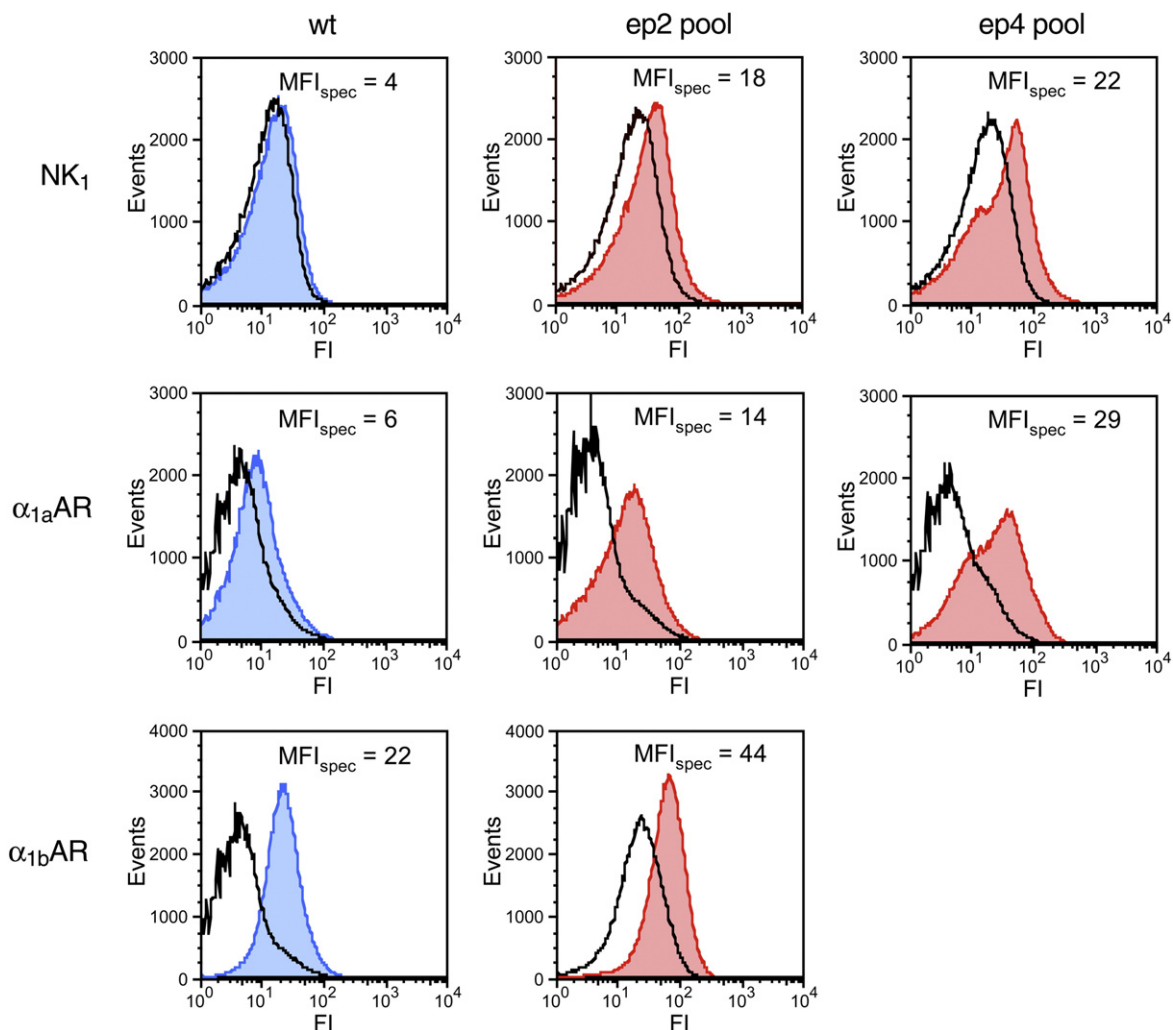


**Fig. 1.** Evolution of functional expression for the three receptors  $NK_1$ ,  $\alpha_{1a}AR$ , and  $\alpha_{1b}AR$ . The fluorescence distribution is shown for cells expressing the wt receptors (blue histograms) and for pools of evolved cells expressing a collection of mutant receptors (red histograms) after two or four rounds of evolution (ep2 pool or ep4 pool, respectively). One round of evolution consists of random mutagenesis followed by four to six rounds of selection by FACS.  $\alpha_{1b}AR$  was evolved for two rounds only (ep2 pool). The expression signal, indicated as the specific mean fluorescence intensity ( $MFI_{spec}$ ), is obtained by subtracting the background MFI (unfilled histograms) from the total MFI (colored histograms) of cells labeled with fluorescent ligand. The unfilled histograms were obtained by competing the fluorescent ligand with a molar excess of unlabeled ligand.

represents a more than 10-fold increase in expression compared to wt  $NK_1$  (Supplementary Fig. 1a).

#### Expression level of evolved $\alpha_{1a}AR$ s

The evolution of  $\alpha_{1a}AR$  also started from a wt cDNA that was expressed at only about 350 receptors/cell. In total, we evolved  $\alpha_{1a}AR$  for four rounds. After two rounds of evolution (ep2 pool), we found that the best receptor variants expressed about 10-fold better than wt  $\alpha_{1a}AR$  (Supplementary Fig. 1b). After two additional rounds of evolution, expression increased further, and the best clones expressed up to 6500 receptors/cell, which is

about 18-fold better than wt  $\alpha_{1a}AR$  (Supplementary Fig. 1b).

#### Expression level of evolved $\alpha_{1b}AR$ s

$\alpha_{1b}AR$  is a close homolog of  $\alpha_{1a}AR$ , and we found that wt  $\alpha_{1b}AR$  was expressed at a relatively high level, namely,  $\sim 2000$  receptors/cell. To our knowledge, this represents the highest functional expression level in *E. coli* for any wt GPCR studied thus far. After two rounds of evolution (ep2 pool), we isolated clones that expressed up to 4000 receptors/cell, which is twofold better than wt  $\alpha_{1b}AR$  (Supplementary Fig. 1c).

### A new 96-well stability screening method for identifying receptors with increased thermal stability

Achieving high expression levels of a correctly folded GPCR located in the membrane is the first critical step in the process of producing sufficient amounts of functional protein for biophysical and structural studies. The second equally important step toward this goal consists of extracting the intact receptor from the membrane lipid bilayer by the help of detergents and maintaining the receptor in a folded and functional state in detergent micelles. The parameter that determines the success of this second step most decisively is receptor stability (we define “stability” here simply as the molecular property of the protein to maintain a correctly folded and active conformation in detergent-solubilized form). In the present study, we wished to readily identify receptor variants showing increased stability among the receptor variants that had been evolved for increased expression. While our prior results suggest that these two properties may be evolved in parallel,<sup>12</sup> they are clearly not identical, and thus, a separate screening step is necessary.

Because we wanted to screen the stability of as many receptor variants as possible, we had to revise the conventional protocol for stability screening, which involves the individual solubilization of receptors followed by LBAs. In the conventional stability assay, each receptor sample has to be processed by a small size-exclusion spin column to separate bound from unbound ligand and assess the

ligand binding signal, since solubilized receptor cannot be quantitatively bound to filters. This spin column step cannot be performed in a 96-well assay format and therefore strongly limits the assay throughput. The key feature of our new stability screening method is the immobilization of biotinylated receptor on streptavidin-coated paramagnetic beads (Fig. 2). For this purpose, we have fused an AviTag to the C-terminus of the GPCR, which is located in the cytoplasm and enzymatically biotinylated in *E. coli* even at wt levels of the BirA protein. Thereby, cells can be exposed to particular detergents to be tested, and solubilization efficiency and stability in detergent can be screened at the same time. Through immobilization of the solubilized receptor, all essential experimental steps of the stability assay—purification, heat treatment, and LBA—can be performed with small receptor amounts and in a highly parallelized format. Immobilized receptor can easily be separated from detergent-solubilized lysates of whole cells by magnetic force, which yields highly concentrated and partially purified receptor preparations. Most importantly, magnetic capturing allows for an efficient separation of bound from free radioligand in the LBA, which avoids the handling of size-exclusion spin columns. All essential steps can therefore be performed in a 96-well assay format. Since the detergent can also be conveniently exchanged and since the beads with immobilized receptor can be exposed to higher temperature, a very general parallel screening system for solubilization, detergent compatibility, and stability of receptor mutants is obtained.

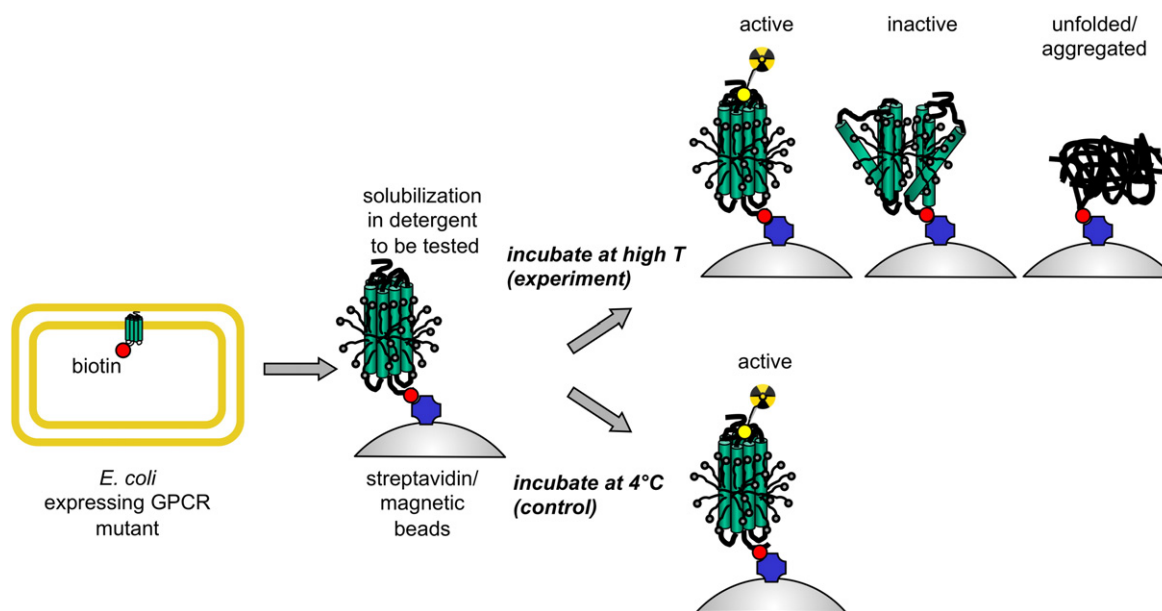


**Fig. 2.** Schematic representation of the new stability assay. See [Results](#) and [Materials and Methods](#) for a detailed description of the stability assay.



Thermal stability of individual evolved receptors was screened after receptor solubilization in the detergent mixture dodecyl- $\beta$ -D-maltopyranoside (DDM)/3-[(3-cholamidopropyl)dimethylammonio]propanesulfonic acid (CHAPS)/cholesteryl hemisuccinate (CHS) followed by a partial purification step using immobilization on streptavidin-containing magnetic beads. Stability was measured as follows: one receptor sample was exposed to a fixed, elevated screening temperature for 20 min, and a second sample was kept on ice. Both of the samples were then assayed for their content of folded receptor by a radioligand binding assay. For ranking the stability of individual evolved receptor variants, we define the stability index (SI) as the ratio between the residual binding signal of the heated sample and the initial binding signal of the sample kept on ice. The screening temperature was chosen individually for each of the three receptor targets. It was chosen to be close to the  $T_m$  of the wt receptors ( $T_m$  is defined as the temperature at which a receptor retains 50% of the initial binding signal after heating at this temperature for 20 min).

We found significant differences in the thermal stability of the three wt receptors, and therefore, we screened the corresponding evolved receptor variants as follows: wt  $\alpha_{1a}$ AR was the most stable wt receptor, and we screened evolved  $\alpha_{1a}$ AR variants at 42 °C. wt  $\alpha_{1b}$ AR, although five times better expressed than its close homolog  $\alpha_{1a}$ AR, was less stable, and we screened evolved  $\alpha_{1b}$ ARs at 36 °C. For wt NK<sub>1</sub> we could not determine the thermal stability because it was not possible to measure a specific binding signal after receptor solubilization. Instead of wt NK<sub>1</sub> we thus decided to use the evolved receptor NK1-C0 to define the screening temperature. Clone NK1-C0 was chosen because it can be functionally solubilized at sufficient amounts and it deviates from the wt NK<sub>1</sub> sequence by only four amino acid substitutions. Based on the thermal stability of clone NK1-C0, we performed the screen of evolved NK<sub>1</sub> receptors at 31 °C.

We initially screened 200 to 300 evolved receptors for each of the three receptor targets by applying the new stability screening method described above. The measurements were then repeated with a subset of receptors to confirm the SI of the most stable receptor variants from the initial screen. The SIs measured by this new stability screening method appear to be highly reproducible, as evidenced by comparing three independently performed screens on a subset of evolved NK<sub>1</sub> receptors (Supplementary Fig. 2).

#### Stability screening of evolved NK<sub>1</sub> receptors

The pool of evolved NK<sub>1</sub> receptors was of special interest. Since it is not possible to obtain any

functionally solubilized receptor for wt NK<sub>1</sub>, one of the main goals of this study was to demonstrate the ability of evolving stable NK<sub>1</sub> variants, which can be functionally solubilized in detergent micelles. We measured the stability of evolved NK<sub>1</sub> receptors of the ep4 pool at 31 °C and found a broad distribution of SIs among the screened clones. Since it is not possible to compare these data to the stability of wt NK<sub>1</sub>, we compared the evolved receptors to the evolved clone NK1-C0, which was closest in sequence to the wt. We found that most evolved receptors of the ep4 pool were more stable than NK1-C0. Notably, the most stable receptor (NK1-E11) showed an SI of 91% compared to 31% for NK1-C0 and 0% for wt NK<sub>1</sub>. To analyze how receptor stability relates to expression level, we plotted the stability data as a function of receptor expression (Fig. 3a). We found that although the data are only loosely correlated, there are many clones that are both highly expressed and more stable. Most importantly, while wt NK<sub>1</sub> cannot be functionally solubilized at all, many of the evolved receptors can be functionally solubilized.

#### Stability screening of evolved $\alpha_{1a}$ ARs

Our initial screen of evolved  $\alpha_{1a}$ ARs was performed on clones that had been evolved for four rounds (ep4 pool). However, we found that about half of these receptors could not be immobilized on streptavidin-coated paramagnetic beads due to the presence of a premature stop codon in their C-terminal receptor sequence. Interestingly, this subset of shortened receptors, which are also lacking the C-terminal fusion adduct TrxA-AviTag, showed about double the expression level than the full-length receptors, which explains their enrichment in the ep4 pool. Because of this high number of shortened receptors in the ep4 pool, we decided to return to the ep2 pool for stability screening, in which C-terminal shortening was negligible. By screening the  $\alpha_{1a}$ AR ep2 pool at 42 °C, we found a broad distribution of SIs, ranging from 34% to 96% (SI of  $\alpha_{1a}$ AR was 56%) (Fig. 3b). The most stable evolved receptors showed great stability, with only little reduction in ligand binding signal after the heat treatment (SI of 96%). Plotting the stability data as a function of expression level reveals that many of the better-expressed receptor variants are also more stable than wt  $\alpha_{1a}$ AR (Fig. 3b). While the quantitative correlation between the two evolved properties is rather weak, it is remarkable that most mutants, which were selected for higher expression level, are at least as stable as the wt, and many are much more stable (Fig. 3). Overall, the results of  $\alpha_{1a}$ AR reveal that the biophysical properties of a weakly expressed but relatively stable receptor can further be improved by applying the method of random mutagenesis and selection by FACS.

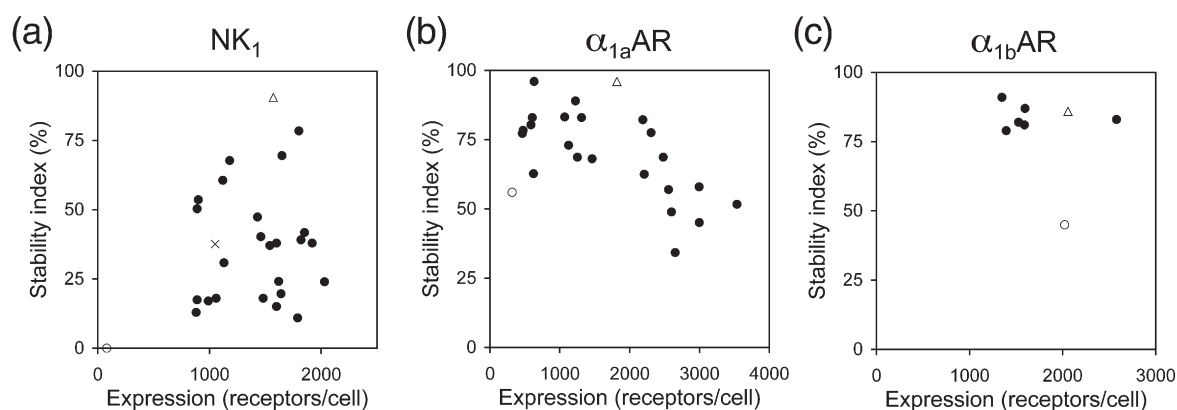


**Fig. 3.** Correlation between thermal stability and expression level for evolved receptors of NK<sub>1</sub>,  $\alpha_{1a}$ AR, and  $\alpha_{1b}$ AR. To measure thermal stability, we exposed solubilized receptors to a fixed temperature for 20 min. The SI indicates the fraction of receptors that retain their ability to bind ligand after the heating step. The thermal stabilities and the expression levels of wt receptors (○) are given as a reference point for the evolved receptors (●). The evolved receptors that we have chosen to characterize in more detail (NK1-E11, A1a-05, and A1b-C10) are indicated (Δ). (a) Stability of evolved NK<sub>1</sub> receptors of the ep4 pool. The samples were heated at 31 °C for 20 min. wt NK<sub>1</sub> cannot be functionally solubilized, and its stability index is set to 0%. As an alternative reference point, we show the evolved clone NK1-C0 (×), which is well expressed and shows only four amino acid substitutions compared to wt NK<sub>1</sub>. (b) Stability of evolved  $\alpha_{1a}$ ARs of the ep2 pool. The samples were heated at 42 °C for 20 min. (c) Stability of evolved  $\alpha_{1b}$ ARs of the ep2 pool. The samples were heated at 36 °C for 20 min.

#### Stability screening of evolved $\alpha_{1b}$ ARs

The stability screen of the evolved ep2 pool of  $\alpha_{1b}$ AR revealed the same limitation as observed for the evolved ep4 pool of  $\alpha_{1a}$ AR; namely, that many of the evolved clones showed a premature stop codon in their C-termini. Stability screening could therefore only be done on a limited number of evolved receptors. For the receptors that could be assayed, the SI was higher than for wt  $\alpha_{1b}$ AR (Fig. 3c shows the most stable clones of this screen).

The enrichment of stop codons in the evolved receptor pools of both adrenergic receptor targets,  $\alpha_{1a}$ AR and  $\alpha_{1b}$ AR, indicates a strong selection in favor of shortened C-termini, which leads to higher expression levels. Despite the problems with shortened C-termini, we could validate the new stability screening method on three different wt receptors. For each receptor, we could isolate many evolved receptors that showed higher functional expression levels as well as higher thermal stability than the wt receptors.

#### Detailed characterization of well-expressed and stable receptors

After we had identified evolved receptors that were well-expressed and more stable than the wt receptors, we went on to characterize the properties of the best receptor variants in more detail. First, we quantified the increase in stability by measuring thermal stability curves, and second, we examined their ligand binding properties.

To quantify the increase in stability of individual receptor variants, we also used the new stability assay setup to measure thermal stability curves (Fig. 4). For this purpose, rather than exposing solubilized receptor to only two different temperatures, we exposed it to a range of temperatures in a gradient thermocycler, typically spanning 40 °C. The stability curve thus allows one to calculate the midpoint of denaturation ( $T_m$ ) for each receptor, which we define as the temperature at which a given receptor retains 50% of its initial ligand binding when heated for 20 min.

The most stable evolved receptor identified among the NK<sub>1</sub> receptors—clone NK1-E11—showed a  $T_m$  of 44.6 °C (Fig. 4a). The stability of NK1-E11 stands in stark contrast to wt NK<sub>1</sub>, which could not be solubilized at all. The evolved receptor NK1-C0, which served as an alternative reference point in the stability screens, showed a  $T_m$  of 27.6 °C. In the stability screen of evolved  $\alpha_{1a}$ ARs, we identified clone A1a-05 as the most stable receptor. Clone A1a-05 showed a  $T_m$  of 50.9 °C, which is 6 °C more stable than wt  $\alpha_{1a}$ AR ( $T_m$  = 44.8 °C), as seen in Fig. 4b. Interestingly, the increase in stability by 6 °C can be traced back to one single mutation, namely, F312L. Introducing this mutation into wt  $\alpha_{1a}$ AR results in a receptor that is as stable as the evolved clone A1a-05 (data not shown). For the evolved  $\alpha_{1b}$ ARs, we chose to characterize clone A1b-C10 in more detail because it showed a strong increase in thermal stability and it deviates from wt  $\alpha_{1b}$ AR by only three amino acid mutations. Clone A1b-C10 showed a  $T_m$  of 48.8 °C, which is 11 °C more stable than wt  $\alpha_{1b}$ AR (Fig. 4c).

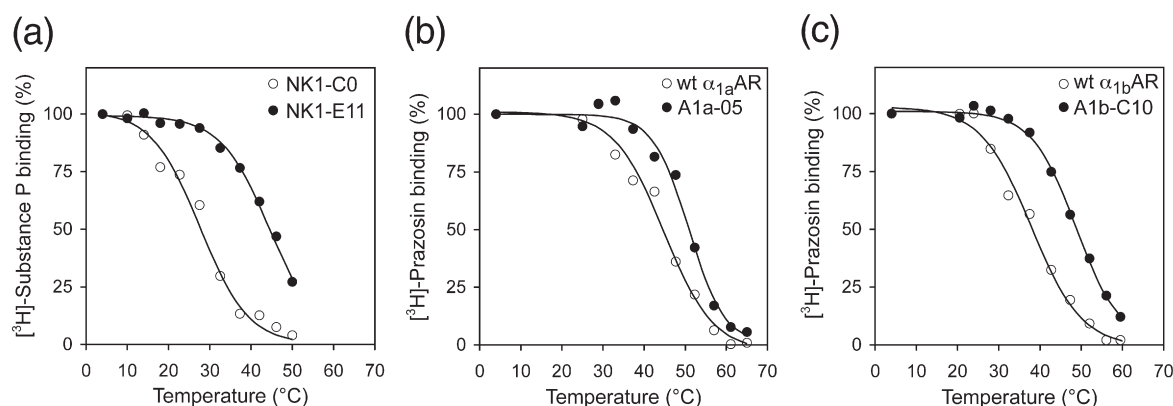


**Fig. 4.** Stability as a function of temperature for evolved receptors NK1-C0, NK1-E11, A1a-05, and A1b-C10. The curves were obtained by heating solubilized receptor at different temperatures for 20 min and measuring the remaining radioligand binding signal. (a) Clone NK1-E11 was the most stable receptor of the NK<sub>1</sub> selection. Since wt NK<sub>1</sub> cannot be functionally solubilized, clone NK1-C0 is shown as a reference point. (b and c) Both the evolved  $\alpha$  adrenergic receptors A1a-05 and A1b-C10 (●) show higher stability than the respective wt receptors (○).

We then analyzed the ligand binding properties of the evolved clones NK1-E11, A1a-05, and A1b-C10 in whole *E. coli* cells with the receptors functionally expressed in the inner membrane. The NK<sub>1</sub> clone NK1-E11 had been evolved by using a fluorescent analog of the agonist Substance P. Saturation binding curves using radioactively labeled [<sup>3</sup>H] Substance P reveal that the evolved clones NK1-E11 and NK1-C0 retain high affinity for Substance P, similar to wt NK<sub>1</sub> (Fig. 5). In contrast to the agonist

Substance P, which binds with similar affinity to the receptors, the antagonist L-732,138 shows approximately 100-fold reduction in affinity for NK1-E11 and NK1-C0 compared to wt NK<sub>1</sub> (Fig. 5d). Similar results were obtained for the evolved adrenergic receptors A1a-05 and A1b-C10, which had been evolved using a fluorescent analog of the antagonist prazosin. Although the affinity of [<sup>3</sup>H]prazosin for the evolved receptors A1a-05 and A1b-C10 was reduced 3- to 4-fold compared to their wt receptors,

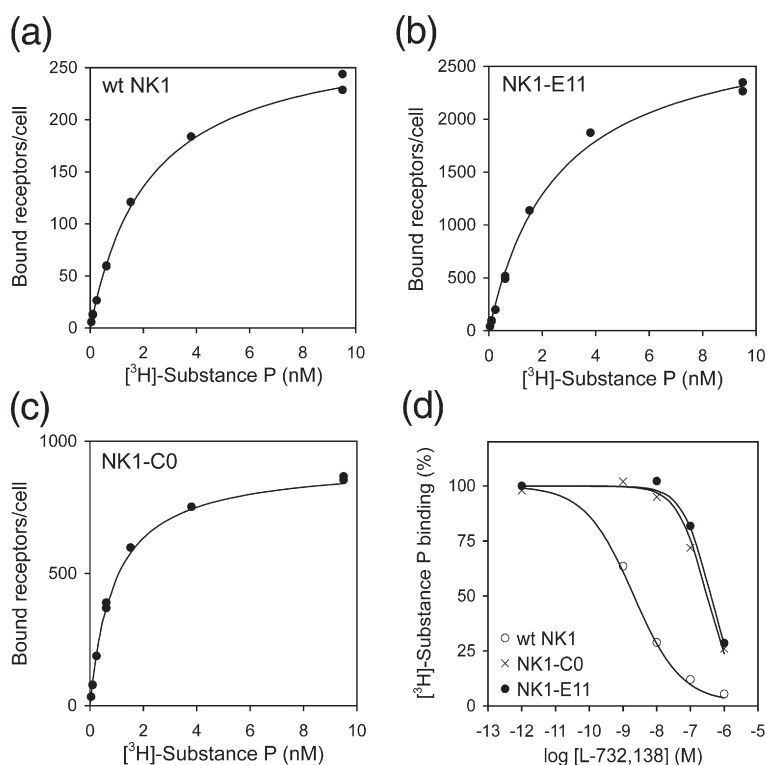


**Fig. 5.** Binding of agonist or antagonist to the evolved NK<sub>1</sub> receptors in comparison to wt NK<sub>1</sub>. (a-c) The curves show receptor occupancy as a function of radioligand concentration. The evolved clones NK1-E11 and NK1-C0 largely retain the wt-like binding affinity for the agonist [<sup>3</sup>H] Substance P. The equilibrium dissociation constants ( $K_d$ ) for the different receptors are  $2.2 \pm 0.2$  nM (wt NK<sub>1</sub>),  $2.6 \pm 0.2$  nM (NK1-E11), and  $0.9 \pm 0.03$  nM (NK1-C0). The functional expression level of NK1-E11 is 10 times higher than that of wt NK<sub>1</sub>. (d) The evolved receptors were also probed for binding of the antagonist L-732,138 by letting the antagonist compete for binding with agonist [<sup>3</sup>H]Substance P (2 nM). The evolved receptors retain the ability to bind antagonist L-732,138, although the affinity is roughly 100-fold lower compared to wt NK<sub>1</sub>.

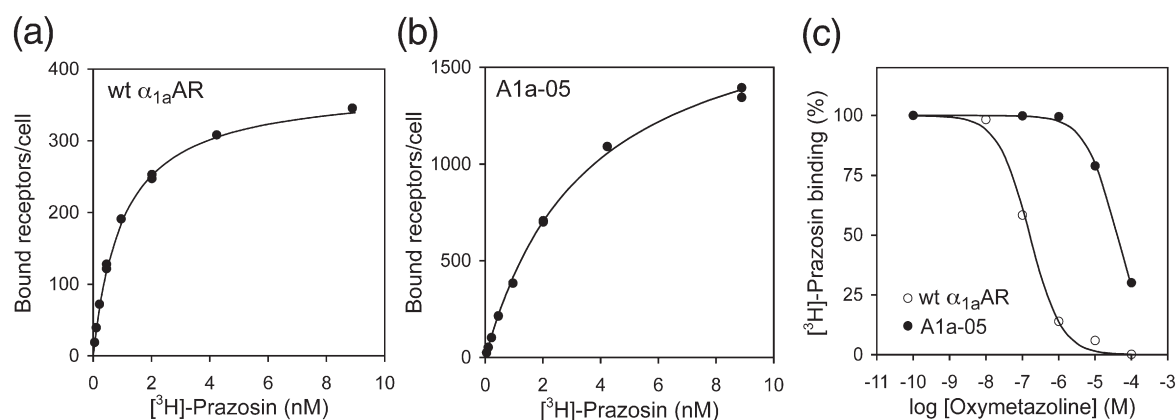


**Fig. 6.** Binding of agonist or antagonist to the evolved clone A1a-05 compared to wt  $\alpha_{1a}\text{AR}$ . (a and b) The curves show receptor occupancy as a function of radioligand concentration. The evolved clone A1a-05 shows a 4-fold lower affinity than wt  $\alpha_{1a}\text{AR}$  for the antagonist  $[^3\text{H}]\text{prazosin}$  ( $K_d$  values are  $3.5 \pm 0.2$  nM and  $0.95 \pm 0.04$  nM, respectively). Its functional expression level is increased 5-fold. (c) Clone A1a-05 also retains affinity for the agonist oxymetazoline. However, compared to wt  $\alpha_{1a}\text{AR}$ , approximately 100-fold higher concentrations of agonist oxymetazoline are necessary to displace antagonist  $[^3\text{H}]\text{prazosin}$  (2 nM).

they still bound prazosin with a  $K_d$  in the low nanomolar range (Figs. 6 and 7). In contrast to the antagonist prazosin, for which the high affinity was largely retained, the affinity of the agonist oxymetazoline for the evolved receptors was reduced approximately 100-fold compared to the wt receptors (Figs. 6d and 7c).

In summary, the ligand binding data show that a given evolved receptor largely retains its wt-like affinity for the ligand that was used for evolving the receptor by FACS-based directed evolution. These results underline our observation that when we select the most fluorescent cells by FACS, we indeed evolve receptors showing increased functional

expression rather than higher affinity for the fluorescent ligand.

The saturation binding data shown in Figs. 5, 6, and 7 also allow us to more accurately quantify the functional expression level of the evolved receptors. In addition to the  $K_d$ , nonlinear fitting of the saturation binding data yields an accurate estimate for the total number of functionally expressed receptors per cell. Based on these measurements, clone NK1-E11 is expressed at 3000 receptors/cell (10-fold better than wt NK<sub>1</sub>), clone A1a-05 is expressed at 1900 receptors/cell (5-fold better than wt  $\alpha_{1a}\text{AR}$ ), and clone A1b-C10 is expressed at 3400 receptors/cell (1.3 times better than wt  $\alpha_{1b}\text{AR}$ ).

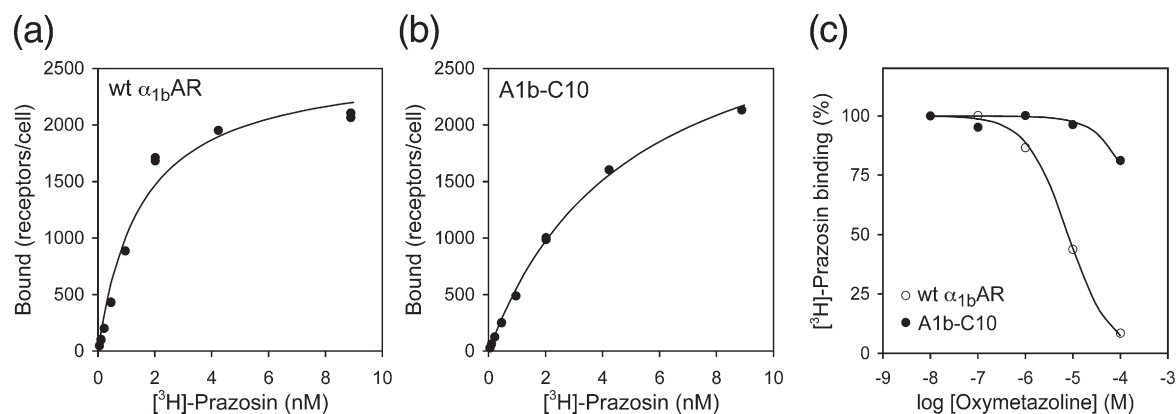


**Fig. 7.** Binding of agonist or antagonist to the evolved clone A1b-C10 compared to wt  $\alpha_{1b}\text{AR}$ . (a and b) The curves show receptor occupancy as a function of radioligand concentration. The evolved clone A1b-C10 shows a 3-fold lower affinity than  $\alpha_{1b}\text{AR}$  for the antagonist  $[^3\text{H}]\text{prazosin}$  ( $K_d$  values are  $4.9 \pm 0.4$  nM and  $1.5 \pm 0.3$  nM, respectively). Its functional expression level is moderately increased. (c) Clone A1b-C10 also retains affinity for the agonist oxymetazoline. However, compared to wt  $\alpha_{1b}\text{AR}$ , approximately 100-fold higher concentrations of agonist oxymetazoline are necessary to displace antagonist  $[^3\text{H}]\text{prazosin}$ .



These numbers correspond to about 1 mg of functional and thermostable GPCR (not counting the fusion proteins present within the expression construct) expressed per liter of *E. coli* shake flask culture.

### Relating the evolved mutations to increased expression and stability

To identify mutations that led to the strong increase in expression and stability, we examined the amino acid sequences of the evolved receptors. To gain further structural and mechanistic insight into how these mutations may influence expression and stability, we mapped them onto the crystal structure of the  $\beta_2$  adrenergic receptor (Fig. 8).<sup>6</sup>

#### Evolved mutations in NK<sub>1</sub>

We sequenced single clones after two and four rounds of evolution (ep2 pool and ep4 pool, respectively). After two rounds of evolution, the highest expressed sequences show  $7 \pm 2$  (SD) amino

acid substitutions per receptor (the evolved mutations are summarized in [Supplementary Fig. 3a](#)). The sequences are diverse, and the mutations are distributed over the entire receptor. There are two strong consensus mutations, I204T and T222R, and both are located in transmembrane helix (TM) 5. Because of their high enrichment in the ep2 pool, they are likely to be critical for increasing receptor expression. The I204T mutation in TM5 is located in a region surrounded by TM3 and TM4 in the ligand binding crevice. It is not unreasonable to speculate about a role of the Thr204 OH group in an H-bond. The second consensus mutation, T222R, is located at the cytoplasmic end of TM5 and points into the solvent. The increase in expression may arise because the positive charge of Arg222 may lead to an optimization of the ionic interaction energy between the receptor and the negatively charged phospholipid head groups of the membrane bilayer. Arg222 would satisfy the positive-inside rule.<sup>16,17</sup>

The selected sequences, after four rounds of evolution (ep4 pool), show  $11.6 \pm 2.8$  (SD) amino acid mutations per receptor, which are distributed over the entire receptor (the evolved mutations are

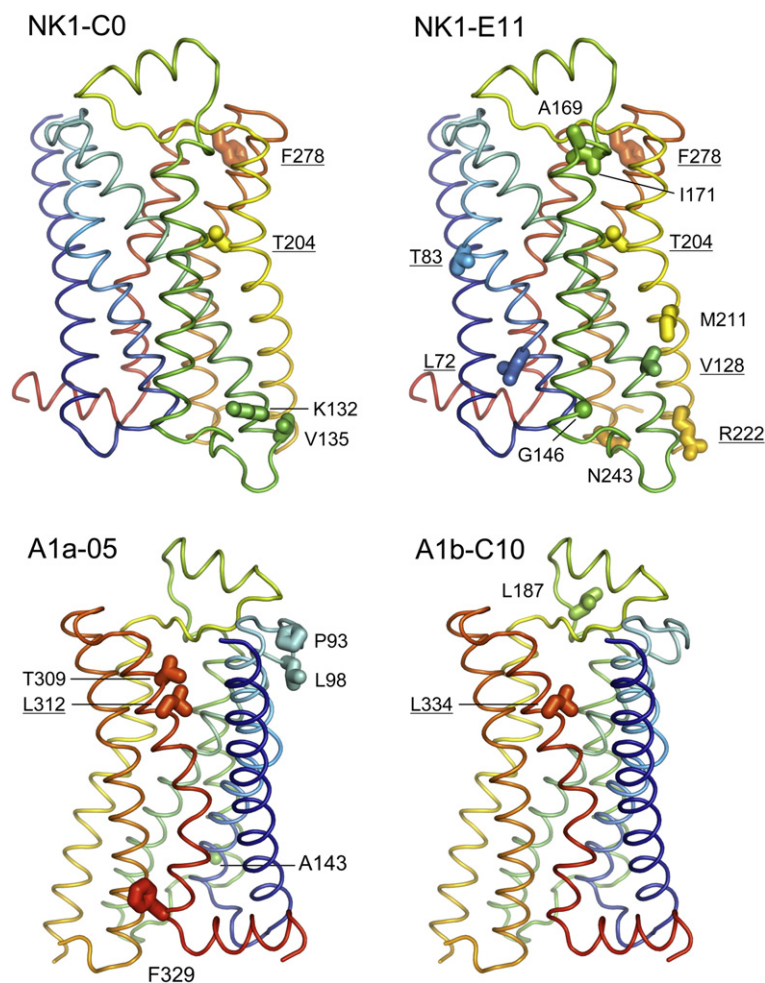


**Fig. 8.** Mutations of the four evolved receptors (NK1-C0, NK1-E11, A1a-05, and A1b-C10) mapped onto the 7TM fold. The crystal structure of the  $\beta_2$  adrenergic receptor was used as a structural template (Protein Data Bank code 2rh1). Underlined mutations correspond to consensus mutations in the corresponding pool of evolved receptors (consensus mutations are defined as those occurring in more than 50% of the evolved receptor sequences shown in [Supplementary Figs. 3, 4 and 5](#)).



summarized in [Supplementary Fig. 3a](#)). In addition to the two consensus mutations I204T and T222R, which were already present in the ep2 pool, four more mutations in different parts of the receptor are strongly enriched (V72L, A83T, F128V, and V247I). Because their occurrence is not restricted to the most stable clones in this pool, these consensus mutations seem to further augment receptor expression levels rather than increase stability.

To identify mutations that strongly increase the stability of the NK<sub>1</sub> receptor, we looked for unique mutations in the 7TM portion (excluding the N- and C-termini) of the most stable evolved clones. The most stable clone, NK1-E11, shows two mutations, A146G and V211M, which do not occur in any other sequence. A146G is located at the cytoplasmic end of TM3, and V211M is located in the middle of TM5. Mapping the mutations on the crystal structure of  $\beta_2$ AR shows that both of them are located on the outside faces of the helices and point into the lipid bilayer ([Fig. 8](#)). In addition, clone NK1-E11 features the K243N mutation, which is also present in other very stable clones. K243N is located at the cytoplasmic end of TM6.

In addition to clone NK1-E11, we identified the clones NK1-H04, NK1-D10, and NK1-B02 as very stable NK<sub>1</sub> variants ([Supplementary Fig. 3b](#)). The following mutations occur exclusively in these stabilized clones: V51M, A93G, T124M, G166A, I191T, and N309D. The location of Met124 in TM3 suggests that it could interact with the conserved helix kink introduced by Pro208 in TM5. Interestingly, Met124 in clone NK1-B02 and the methionine of the V211M mutation in the most stable clone, NK1-E11, although separated in the sequence and located on different TM helices, are adjacent in the receptor tertiary structure. Both methionine side chains point into the same interface region located between TM3 and TM5. This could suggest a critical role in receptor stability for this region in the NK<sub>1</sub> receptor. Others have made similar observations: the stability and the expression level could be strongly increased for the  $\beta_2$  adrenergic receptor by single-point mutations in the helical interface between TM3, TM4, and TM5.<sup>18</sup>

### Evolved mutations in $\alpha_{1a}$ AR

To analyze which mutations led to an increase in expression and stability in the evolution of  $\alpha_{1a}$ AR, we sequenced single clones of the ep2 pool, which correspond to the data points shown in [Fig. 3b](#). There are, on average,  $6.9 \pm 2.2$  (SD) amino acids per receptor. The sequences are diverse, and the mutations are distributed over the entire receptor (the evolved mutations are summarized in [Supplementary Fig. 4](#)).

There are several mutations that occur with high frequency in the evolved  $\alpha_{1a}$ ARs, and from the

sequencing data alone, we would expect that they are responsible for the improved properties of the evolved receptors. The most prominent of these consensus mutations is found at position 14 in the N-terminus of the receptor. In 96% (22/23) of the evolved sequences, the wt Cys residue at position 14 is mutated to amino acid Tyr, Phe, Ser, or Arg, which are all accessible by a single nucleotide exchange. We analyzed the effect of this “cys-escape” mutation by replacing Cys at position 14 with a Tyr in wt  $\alpha_{1a}$ AR. While the expression level of this single-point mutant went up about 3.5-fold, neither the affinity for prazosin nor the receptor stability was altered (data not shown). This increase in expression is likely to be related to the elimination of Cys rather than the introduction of Tyr at position 14. The elimination of Cys14 may prevent the formation of nonspecific intramolecular or intermolecular disulfide bonds in the oxidizing periplasm of *E. coli*. Cys99 in TM3 and Cys176 in EL2 form the putative disulfide bond conserved in practically all GPCRs, and both are close enough to be potentially attacked by Cys14. It is worth noting that the closely related receptor subtype  $\alpha_{1b}$ AR shows a Ser residue instead of Cys at the homologous position, which may in part explain the higher expression level of wt  $\alpha_{1b}$ AR compared to wt  $\alpha_{1a}$ AR.

The second most frequent consensus mutation enriched in the ep2 pool of the  $\alpha_{1a}$ AR evolution is F312L. It is located in TM7 and points into the ligand binding crevice. Since the presence of F312L is strongly correlated with an increase in stability ([Supplementary Fig. 4](#)), we analyzed its effect on expression, stability, and ligand binding affinity by characterizing the single-point mutant F312L in the wt  $\alpha_{1a}$ AR background (data not shown). The F312L mutation led to a twofold increase in expression, and the thermal stability was increased by 6 °C compared to wt  $\alpha_{1a}$ AR. However, the F312L mutation decreased the affinity for the antagonist [<sup>3</sup>H]prazosin by approximately fivefold to sixfold. Interestingly, this Phe-to-Leu mutation was also strongly enriched at the homologous position in evolved  $\alpha_{1b}$ ARs (corresponding to the F334L mutation in  $\alpha_{1b}$ AR, see below), and the occurrence of F334L is correlated with increased stability in those receptors as well.

Besides the two strong consensus mutations mentioned above (C14[YFSR] and F312L), two additional consensus mutations (N322K and N318H) occur in the ep2 pool of  $\alpha_{1a}$ AR, and they are associated with the highest expressed clones (but not with the most stable ones). Both mutations are located in TM7, in a region of the receptor that is known to form a highly interconnected hydrogen-bonding network.<sup>19</sup> In the crystal structures of solved GPCR structures, this network is composed of highly conserved residues located in TM1, TM2, and TM7 and several molecules of structural water.<sup>4–10</sup>

### Evolved mutations in $\alpha_{1b}$ AR

To analyze the mutations leading to increased stability of  $\alpha_{1b}$ AR, we sequenced seven of the most stable clones of the ep2 pool. These clones correspond to the data points in Fig. 3c. On average, they show  $5.9 \pm 1.7$  (SD) amino acid substitutions per receptor (the evolved mutations are summarized in Supplementary Fig. 5). The mutations are diverse, and they are distributed over the entire receptor. Interestingly, all of these stable clones show the F334L consensus mutation, which is homologous to the stabilizing F312L mutation enriched in the stable receptor variants of  $\alpha_{1a}$ AR. This stabilizing Phe-to-Leu mutation was therefore evolved convergently in the two independent selections of both  $\alpha$  adrenergic receptor subtypes.

It is worth emphasizing again that an additional type of mutation was strongly enriched in a subset of evolved receptors of both  $\alpha_{1a}$ AR and  $\alpha_{1b}$ AR, namely, premature stop codons in the C-termini of the receptors. Receptors showing these stop codons were found among the best expressed clones. For  $\alpha_{1a}$ AR, stop codons are found at position Lys349, and for  $\alpha_{1b}$ AR, it is at position Cys384, which are both beyond helix 8 in the presumably unstructured region. In both instances, the stop codons lead to premature termination of translation such that the major part of the receptor C-terminus—including the fusion adduct TrxA-AviTag—is not translated. The truncations of the relatively long C-termini of  $\alpha_{1a}$ AR and  $\alpha_{1b}$ AR seem to increase expression about twofold even though the TrxA fusion adduct, which is thought to increase expression,<sup>13</sup> is missing (Supplementary Fig. 1b, see the best-expressing clones in the ep4 pool of  $\alpha_{1a}$ AR). The fact that premature stop codons occur in the C-termini, but not within the 7TM domains of the receptors, emphasizes one of the major strengths of evolving higher-expressing receptors by FACS-based directed evolution: because we use the binding of fluorescent ligand as a stringent selection criterion during receptor evolution, the structural integrity of the 7TM fold remains conserved.

## Discussion

The inability to express GPCRs at high levels and their limited stability in detergent micelles restrict the process of crystallization and structure determination. To overcome these restrictions, we have developed a directed evolution method that allows the rapid identification of mutations in a receptor sequence that lead to higher functional expression and higher stability. In a previous study, we have demonstrated the feasibility of the method on the model protein neurotensin receptor NTR1,<sup>12</sup> where we had found that the enriched mutations positively

affected both expression and stability. In the present study, we further validated the method by applying it successfully to three additional human GPCRs of the rhodopsin family. Since the NTR1 wt is already expressed at relatively high levels in *E. coli*, we wanted to test if GPCRs could be evolved for higher expression even if their wt expression level is much lower. We also wanted to establish how well higher expression level and higher biophysical stability in detergent-solubilized form are correlated.

### Increasing expression and stability

The present study shows that the functional expression level of even very weakly expressing wt GPCRs can be strongly increased by directed evolution. The relative increase in expression was especially high for the evolved receptors of NK<sub>1</sub> and  $\alpha_{1a}$ AR, both of which show very weak heterologous wt expression in *E. coli*. For NK<sub>1</sub>, we could evolve receptors that express more than 10-fold better ( $\sim 3000$  receptors/cell) than the wt receptor. For  $\alpha_{1a}$ AR, we isolated receptors expressing more than 10-fold better ( $\sim 3500$  receptors/cell). Even for the relatively well-expressed wt  $\alpha_{1b}$ AR, we isolated receptor variants that expressed better ( $\sim 3500$  receptors/cell), although the further improvement was only moderate. These expression levels correspond to approximately 1 mg/l functional GPCR (excluding the mass of the fusion proteins of the expression construct) at a cell density of OD<sub>600</sub>=5 and are in the range of the requirements for structural studies. It is interesting to note that a similar final level is reached for all three receptors, as well as for the evolved NTR1 ( $\sim 6000$  receptors/cell), independent of the starting number. It is currently unclear whether this constitutes an intrinsic limit in the *E. coli* biosynthesis of such proteins, but it is at a level that allows very convenient preparation of these proteins for biophysical and structural studies.

While our strategy of mutagenizing the receptor aims at improving functional expression and stability, the FACS-based sorting strategy could also be used to improve the host strain. It is possible that the apparent functional expression limit for GPCRs can be overcome by strain engineering. *E. coli* has been engineered for improved membrane protein expression,<sup>20–22</sup> and it will be interesting to see how general these chromosomal mutations are for membrane proteins or whether different ones are required to improve functional GPCR expression.

In general and in agreement with our previous studies,<sup>12</sup> we found that most receptors that were better expressed were also more stable. While the two variables were only loosely correlated (Fig. 3), it is noteworthy that the SI of many mutants (selected by expression) was higher than the wt. The rapid identification of the most stable receptor variants among the well-expressed ones was enabled by a

newly developed stability screen in a 96-well assay format (Fig. 2). By this screen, we were able to isolate highly stabilized and well-expressed clones such as clone NK1-E11 derived from NK<sub>1</sub>, clone A1a-05 derived from  $\alpha_{1a}$ AR, and clone A1b-C10 derived from  $\alpha_{1b}$ AR, all from the clones that had been selected for higher expression.

The observation that expression and stability are only weakly correlated might be expected, since, during evolution, the mutants are primarily selected for their increased functional expression level rather than biophysical stability directly. However, the data show that increased biophysical stability is an important factor for higher expression—among several other factors that are unrelated to stability. Clearly, to enable structural studies of GPCRs, both properties need to be improved. A receptor, which cannot be expressed, is not useful for structural studies, even if it is intrinsically more stable than the wt receptor. The methods presented in this paper allow the engineering of receptors which are well-expressed and, at the same time, stable.

### Technical aspects of the selection method

In addition to our primary findings discussed above, a note on three further technical aspects may be of interest when discussing the performance of the presented method. First, the method was implemented without making *a priori* assumptions about the structure or the function of the targeted receptor. To initiate the selection process, we simply started from wt cDNA of some receptors, for which fluorescent ligands were commercially available. Genetic manipulations were restricted to the removal of internal restriction sites and did not change the amino acid sequence. The wt receptors were cloned into the expression vector including all of their potentially problematic features such as loops, N- and C-termini, or possible protease sites. To initiate the selection process, it was not necessary to employ classical techniques of expression optimization. The results in this study were obtained by keeping all expression conditions constant.

The second technical aspect addresses the concept of introducing mutations into the receptor for increasing expression and stability. In order to avoid the enrichment of highly expressed but misfolded mutants, we are employing ligand binding as a functional selection criterion. The results show that ligand binding represents a strong selection pressure for the structural integrity of GPCRs. This can be explained by the fact that, for most GPCRs, most pronounced for the ones binding small ligands and peptides, the ligand binding site is contributed by residues from different parts of the receptor, which must be in a particular three-dimensional arrangement. Therefore, the helices and loops must be oriented in a

native-like conformation to provide the functional contacts for ligand binding. Indeed, the evolved receptors typically retain a functional binding site for the ligand that was used for the FACS-based selection process: radioligand binding analysis showed that the evolved receptors bound their cognate ligand with affinity similar to that of the wt receptors. As an exception to this general outcome, we observed that a subset of evolved receptors of  $\alpha_{1a}$ AR and  $\alpha_{1b}$ AR showed the Phe-to-Leu consensus mutation in TM7, which led to a 3- to 4-fold decrease in affinity for prazosin binding. The loss in binding affinity, however, coincided with a considerable gain in receptor stability. In addition, evolved receptors that were selected using an agonist (NK<sub>1</sub> selection) still showed affinity for an antagonist, and evolved receptors that were evolved using an antagonist ( $\alpha_{1a}$ AR and  $\alpha_{1b}$ AR selections) still showed affinity for an agonist. The binding affinity for the nonselected ligand, however, was reduced approximately 100-fold. This might suggest that the ability of wt receptors to bind to one or the other type of ligand with similar affinity comes at the expense of stability.

We are well aware of the fact that selecting for mutations that preserve the ability to bind a ligand does not rule out the possibility of selecting for mutations that affect other important functional features of a GPCR, such as functional coupling to G proteins. In fact, it is very probable that some of the stabilizing mutations do exert their effects by constraining conformational flexibility whereby the equilibrium is shifted toward a more active or more inactive receptor state.

Despite the fact that stabilizing mutations may affect the signaling profile of a mutated GPCR, we believe that restraining conformational flexibility represents a decisive advantage for the structural determination of GPCRs. This has been demonstrated by solving the crystal structure of the turkey  $\beta_1$  adrenergic receptor, which was made possible by introducing six stability-enhancing mutations in the receptor.<sup>7</sup> Similarly, thermal stabilization of bovine rhodopsin by an engineered disulfide bond in bovine rhodopsin has enabled its recombinant production for the first time, as reported in a recent study.<sup>23</sup> The engineered rhodopsin could then be crystallized and its structure solved. Before this stabilizing mutation had been identified, rhodopsin had to be extracted from the bovine retina to obtain sufficient protein for structural studies.<sup>4</sup> More recently, the structure of the chemokine receptor CXCR4 was solved, and again, several stabilizing mutations were necessary to allow its structural determination.<sup>10</sup> Stability engineering of GPCRs therefore seems to emerge as the standard procedure rather than the exception for atomic-resolution structural studies. The methods reported in the present paper enable the fast identification of



mutations that allow the engineering of both receptor expression and stability.

As a third technical aspect of the method, we want to note that the successful selection for higher expression and stability relies on both a strong functional selection criterion (such as ligand binding) and the ability to sample a large sequence space. Sampling the largest sequence space possible increases the chances of isolating the few beneficial mutants among the majority of nonfunctional ones, which inevitably dominate a naïve gene library generated by random mutagenesis. In this study, we routinely analyzed  $10^7$  to  $10^8$  mutant clones per selection round. These numbers were achieved on a high-speed FACS, which analyzes cellular parameters (such as receptor expression) individually for each clone. Our results indicate that the employed library sizes in this study were large enough to sample several different amino acid types at every given position in the sequence. For example, we found that Cys14 in  $\alpha_{1a}$ AR—a residue that strongly limits expression of the wt receptor—was mutated to four different amino acids in the evolved clones (Tyr, Phe, Ser, and Arg) which can be reached by single base substitutions. For this pattern to occur the Cys codon in the naïve library must have been randomized at least at two nucleotide positions to give rise to the selected mutations. Changes in the third position of the Cys codon would have been synonymous (and thus be of unfavorable phenotype selected against), would have introduced a stop codon (which is strongly selected against), or would have introduced Trp, which we did not find.

A further evidence for thorough sampling of the sequence space is the convergent evolution of the Phe-to-Leu consensus mutation in TM7 in two independent selections on the two homologous receptors  $\alpha_{1a}$ AR and  $\alpha_{1b}$ AR. Most importantly, the sampled sequence space was large enough to allow for the identification of very rare but highly beneficial mutations.

### Relating mutations to evolved properties

What mutations make the evolved receptors better expressed and more stable, and what molecular mechanisms may be involved in the improvements? The general conclusion we draw from this study is that there exist many different mutations for a given GPCR sequence that lead to improved expression and stability. For example, we identified mutations that increase expression, but not stability, and do not seem to alter the native tertiary receptor structure at all. This is the case for position Cys14 in the N-terminus of  $\alpha_{1a}$ AR. Replacing Cys14 increases expression about threefold to fourfold without changing the stability or the ligand binding properties of the receptor. The

simplest and most likely explanation for this strong effect is that the elimination of Cys14 prevents the formation of nonnative intramolecular disulfide bonds during co-translational receptor insertion into the membrane. Other mutations such as the Phe-to-Leu mutation in TM7 of  $\alpha_{1a}$ AR or  $\alpha_{1b}$ AR have a beneficial effect on both expression and stability. We have already given an examination of a subset of evolved mutations that we predict as the most relevant ones from statistical analysis and examination of some individual mutants (see [Results](#)). Many of these predictions remain speculative to a certain degree, and it will be necessary to test more mutations individually for their actual quantitative contributions. This information would then enable the engineering of receptors that would profit from combining the best mutations in a single sequence.

## Conclusions

In recent years, there have been several advances in the field of membrane protein engineering. Some of the recently developed techniques aim at improving membrane protein expression levels, for example, by manually screening blots of random mutants, yet without directly screening for function.<sup>24</sup> Other techniques aim at identifying mutations that increase protein stability in detergent micelles. These techniques include the individual functional screening of random mutants<sup>25</sup> or the systematic screening of alanine substitutions.<sup>26</sup> Yet other techniques aim at identifying amino acids that are critical for receptor function and signaling by employing screening assays in yeast.<sup>27–29</sup>

Complementary to such approaches, we have developed a protein engineering platform that allows the evolution of well-expressed and stable GPCRs that retain their functional ligand binding properties. It exploits the power of evolution over several generations, the wide range of possible substitutions, and the semiquantitative evaluation of individual mutants by FACS. The method has now been validated on four different GPCRs of the rhodopsin family. The results in this study show that FACS-based directed evolution of GPCRs represents a nearly assumption-free experimental approach, and it should therefore be generally applicable to other members of the GPCR superfamily.

## Materials and Methods

### Library construction

The three human GPCRs to be evolved were the tachykinin receptor NK<sub>1</sub>,  $\alpha_{1a}$ AR, and  $\alpha_{1b}$ AR. The wt

cDNA encoding the receptors was obtained from the Missouri S&T cDNA Resource Center†. The full-length cDNA (except the ATG start codon) was cloned into a derivative of the expression vector pRG/III-hs-MBP<sup>30</sup> (kindly provided by R. Grisshammer, National Institutes of Health) via the restriction sites BamHI and Cfr9I. This vector encodes an N-terminal fusion of maltose binding protein (MBP) to the receptor and a C-terminal fusion of TrxA. To create genetic diversity, we amplified the DNA encoding the GPCR (excluding the fusion adducts) by error-prone PCR using the GeneMorph II Random Mutagenesis Kit (Stratagene). Ten nanograms of template DNA was amplified by 30 cycles of PCR. The randomized PCR product was further amplified with high accuracy by PCR using Phusion polymerase (Finnzyme) to obtain sufficient amounts of DNA for library size ligation into the expression vector. *E. coli* strain DH5 $\alpha$ -E (Invitrogen) was used for library cloning and expression. Cells were transformed by electroporation. The final library size was  $10^7$  to  $10^8$  transformed clones. Sequencing of single clones of the naïve libraries showed three to four nucleotide substitutions per kilobase of DNA for the NK<sub>1</sub> and  $\alpha_{1a}$ AR libraries and two to three substitutions for  $\alpha_{1b}$ AR libraries (per round of mutagenic PCR). The sequenced clones showed a homogeneous distribution of mutations, including equal amounts of transitions and transversions, which were equally distributed among the four bases. Clonal amplification of the naïve library after electroporation took place at 37 °C in 50 ml 2xYT medium containing 1% glucose. After electroporation, the cells were grown for 1 h at 37 °C, 100  $\mu$ g/ml carbenicillin (Carb) was added, and the cells were grown for another 2–3 h. At this point, the subpopulation of transformed cells, representing a minor fraction of the total biomass, was mechanically separated from the bulk cell mass of non-transformed cells by passing the liquid culture through a 5- $\mu$ m filter (Millipore). By this filtration step, the transformed cells were recovered in the flow-through, while the non-transformed cells, which fail to divide under Carb selection but keep growing to long aggregating filaments, are retained on the filter. The fraction of transformed cells was centrifuged at 5,000g for 5 min, resuspended in 50 ml fresh 2xYT medium containing 1% glucose and 100  $\mu$ g/ml Carb, and grown to an OD<sub>600</sub> of 0.1. The cells were centrifuged at 5,000g for 5 min, resuspended in 1x Hogness modified freezing medium [36 mM K<sub>2</sub>HPO<sub>4</sub>, 13.2 mM KH<sub>2</sub>PO<sub>4</sub>, 0.4 mM MgSO<sub>4</sub>, 1.7 mM Na<sub>3</sub>-citrate, 6.8 mM (NH<sub>4</sub>)<sub>2</sub>SO<sub>4</sub>, and 4.4% (v/v) glycerol], frozen in liquid N<sub>2</sub>, and stored at –80 °C until further use.

### Selection for higher expression

The basic protocol for selecting higher-expressing receptor mutants has been described in detail.<sup>12</sup> In the present study, it was adapted as follows. A frozen library of *E. coli* cells was thawed and grown in 2xYT medium (1% glucose and 100  $\mu$ g/ml Carb) at 37 °C for 2 h. A fresh expression culture in 20 ml 2xYT medium (0.2% glucose and 100  $\mu$ g/ml Carb) was inoculated at OD<sub>600</sub>=0.05, grown at 37 °C to an OD<sub>600</sub>=0.5, and induced with 0.3 mM isopropyl- $\beta$ ,D-thiogalactopyranoside. Expression

took place at 20 °C for 18–24 h. For sorting the libraries by FACS, we diluted the cells into ligand binding buffer (LBB) at  $2 \times 10^8$  cells/ml. For cells expressing the  $\alpha_{1a}$ AR and  $\alpha_{1b}$ AR libraries, the LBB was TKCl (50 mM Tris–HCl, pH 7.4, and 100 mM KCl); for NK<sub>1</sub>, it was 5xPBS-K [50 mM K<sub>2</sub>HPO<sub>4</sub>, 9 mM KH<sub>2</sub>PO<sub>4</sub>, and 0.7 M KCl, pH 7.4 (note that all sodium salts were replaced by potassium salts in this buffer)] supplemented with protease inhibitors (Complete Protease Inhibitors EDTA-free; Roche). The  $\alpha_1$ AR libraries were labeled with 200 nM prazosin-BODIPY-FL (Invitrogen) for 1–2 h on ice. Nonspecific binding was determined by the addition of 10  $\mu$ M unlabeled prazosin (Tocris Bioscience). The NK<sub>1</sub> libraries were labeled with 300 nM Substance P Oregon Green (Invitrogen) for 2–3 h on ice. This compound is NH<sub>2</sub>-RPKPQQFFQLM-CONH<sub>2</sub> with Oregon Green attached to Lys.<sup>3,31</sup> Nonspecific binding was determined by the addition of 10  $\mu$ M unlabeled Substance P (Tocris Bioscience). The cells were washed by centrifugation at 10,000g for 90 s and resuspension in the same volume of TKCl. Sorting was done on a FACSaria II (BD Biosciences) at 20,000–30,000 events/s in yield mode (for sorting naïve libraries) or purity mode (for subsequent sorting rounds). The most fluorescent 0.5–1.5% of the cells in the population ( $10^7$  to  $10^8$  cells) were sorted directly into 2xYT (1% glucose and 100  $\mu$ g/ml Carb) for regrowth and further selection. The most fluorescent cells were enriched by sorting the libraries for three to six rounds by FACS.

### Radioligand binding assay on whole cells

Radioactive ligand binding on whole cells was used to measure the functional surface expression level. Twenty microliters of expression culture was added to 160  $\mu$ l LBB in a 96-well polystyrene plate. The LBB for  $\alpha_1$ AR clones was 50 mM Tris–HCl, 0.1% (w/v) bovine serum albumin (BSA), 1 mM ethylenediaminetetraacetic acid (EDTA), and 40  $\mu$ g/ml bacitracin, pH 7.4, containing 10 nM [<sup>3</sup>H] prazosin (PerkinElmer). Nonspecific binding was determined by the addition of 10  $\mu$ M unlabeled prazosin. The LBB for NK<sub>1</sub> clones was 5xPBS-K supplemented with 0.1% (w/v) BSA, 40  $\mu$ g/ml bacitracin, and Complete Protease Inhibitors containing 10 nM [<sup>3</sup>H]Substance P (PerkinElmer). Nonspecific binding was determined by the addition of 10  $\mu$ M unlabeled Substance P (Tocris Bioscience). After incubation for 2.5–3 h at 4 °C, the bound ligand was separated from the unbound ligand by fast vacuum filtration on 96-well filtration plates with glass fiber filters (MAFBNB; Millipore), and the filters were washed with 1 ml ice-cold TKCl. The filters were transferred to liquid scintillation vials containing 5 ml Optiphase HiSafe 2 scintillation cocktail (PerkinElmer), incubated for 24 h, and counted on a Betamatic II liquid scintillation counter (Kontron). To derive the amount of receptors per cell, we assumed a cell density of  $10^9$  cells/ml per 1 unit of OD<sub>600</sub>. For determining equilibrium binding affinities, we used a dilution series of radioligand (0.1–10 nM). The data were fit to a one-site binding model. For measuring ligand competition binding, we set the radioligand concentration to 2 nM. For  $\alpha_1$ AR clones, the non-labeled competing ligand was the agonist oxymetazoline (Tocris Bioscience); for NK<sub>1</sub> clones, it was the antagonist L-732,138 (Tocris Bioscience). All binding data were analyzed by nonlinear regression using SigmaPlot.

† [www.cdna.org](http://www.cdna.org)



### Screening of thermal stability in a 96-well assay format

A new method for screening the stability of solubilized receptors in a 96-well assay format was developed. It consists of four steps. First, the receptor is expressed and biotinylated *in vivo*. Second, the receptor is solubilized and partially purified by immobilization on streptavidin-coated paramagnetic beads. Third, the receptor is exposed to stability screening conditions that induce receptor unfolding (e.g., heat, detergent, or buffer). Fourth, the amount of residual folded receptor is determined by an LBA after exposing the receptor to the screening conditions.

The detailed protocol is as follows. Biotinylated receptor was expressed using a derivative of the pRG vector that contains a C-terminal AviTag (GLNDIFEAQKIEWHE, biotinylation on K) instead of a deca-His tag. *In vivo* biotinylation took place without adding free biotin to the expression medium and without co-expressing the *E. coli* biotin ligase BirA. Not supplying extra biotin is advantageous for this protocol because free biotin strongly competes with biotinylated receptors for binding to streptavidin during receptor immobilization. After expression, the biotinylated receptor was solubilized and partially purified by immobilization on streptavidin-coated paramagnetic beads as follows: in a 2-ml microcentrifuge tube, a cell pellet corresponding to a 2-ml expression culture was washed once with TKCl and then solubilized in 200  $\mu$ l solubilization buffer containing 50 mM Tris-HCl (pH 7.4), 200 mM NaCl, 30% (v/v) glycerol, 1 mM EDTA, Complete protease inhibitors, 40  $\mu$ g/ml deoxyribonuclease I (Roche), 10 mM MgCl<sub>2</sub>, and detergents [DDM, 1% (w/v); CHAPS, 0.5% (w/v); and CHS, 0.1% (w/v) (all from Anatrace)]. Solubilization took place at 4 °C for 2 h with gentle agitation. Solubilized samples were centrifuged at 20,000g for 20 min to remove cell debris. The supernatant was mixed with 10  $\mu$ l of Dynabeads MyOne Streptavidin T1 beads (Invitrogen) in a 96-well polystyrene plate, and receptor immobilization took place for 2 h at 4 °C with gentle agitation. The samples were transferred to a 96-well PCR plate, and the beads were captured by a 96-well magnetic capturing device (Dyna). The beads were washed twice with 150  $\mu$ l stability assay buffer [50 mM Tris-HCl, 100 mM NaCl, 30% (v/v) glycerol, 1 mM EDTA, Complete Protease Inhibitors, 0.01% (w/v) DDM, 0.5% (w/v) CHAPS, and 0.1% (w/v) CHS] and resuspended in a final volume of 120  $\mu$ l stability assay buffer. Thermal stability was measured by exposing one aliquot of immobilized receptor to a specific temperature in a thermocycler (Biometra) for 20 min; a second aliquot was kept on ice. After cooling the heated receptor on ice, we assayed all samples for their content of folded receptor by an LBA. The immobilized receptor was incubated for 1.5 h on ice with 100  $\mu$ l LBB [50 mM Tris-HCl (pH 7.4), 15% (v/v) glycerol, 1 mM EDTA, 0.1% (w/v) BSA, Complete Protease Inhibitors, 0.01% (w/v) DDM, 0.5% (w/v) CHAPS, and 0.1% (w/v) CHS] containing 10 nM radioligand. The bound ligand was separated from the unbound ligand by magnetic capturing of the beads, removing the supernatant, washing the beads once with 150  $\mu$ l LBB, and resuspending the beads in a final volume of 20  $\mu$ l LBB. The beads were centrifuged at 2,000g for 2 min and resuspended by sonication for 10 s in a water bath. Scintillation was counted in 200  $\mu$ l OptiPhase

Supermix cocktail (PerkinElmer) on a liquid scintillation counter (1450 Microbeta Plus; PerkinElmer). The nonspecific binding signal was less than 10% of the total signal. The SI for a receptor is defined as the ratio between the residual binding signal of the heated receptor sample and the initial binding signal of the sample kept on ice. For measuring entire stability curves, we exposed 20  $\mu$ l samples of immobilized receptor to a temperature gradient (typically spanning 40 °C) on a gradient thermocycler (Biometra). The data were analyzed by nonlinear regression using SigmaPlot.

### Molecular modeling of the evolved mutations

The crystal structure of the  $\beta_2$  adrenergic receptor (Protein Data Bank code 2rh1) was used to analyze the evolved mutations in a structural context. PyMOL (DeLano Scientific) was used for molecular modeling and visualization.

Supplementary materials related to this article can be found online at [doi:10.1016/j.jmb.2011.02.051](https://doi.org/10.1016/j.jmb.2011.02.051)

### Acknowledgements

We acknowledge the use of and the very professional help by the staff of the Flow Cytometry Laboratory of the Institute for Biomedical Engineering, University of Zurich and Eidgenössische Technische Hochschule Zurich. This work was supported by a predoctoral fellowship to I.D. from the Forschungskredit of the University of Zurich and by the Swiss National Science Foundation (National Center of Competence in Research in Structural Biology) to A.P.

### References

1. Schiöth, H. B. & Fredriksson, R. (2005). The GRAFS classification system of G-protein coupled receptors in comparative perspective. *Gen. Comp. Endocrinol.* **142**, 94–101.
2. Okuno, Y., Tamon, A., Yabuuchi, H., Nijima, S., Minowa, Y., Tonomura, K. *et al.* (2008). GLIDA: GPCR–ligand database for chemical genomics drug discovery—database and tools update. *Nucleic Acids Res.* **36**, D907–D912.
3. Lagerström, M. C. & Schiöth, H. B. (2008). Structural diversity of G protein-coupled receptors and significance for drug discovery. *Nat. Rev., Drug Discov.* **7**, 339–357.
4. Palczewski, K., Kumasaka, T., Hori, T., Behnke, C. A., Motoshima, H., Fox, B. A. *et al.* (2000). Crystal structure of rhodopsin: a G protein-coupled receptor. *Science*, **289**, 739–745.
5. Rasmussen, S. G., Choi, H. J., Rosenbaum, D. M., Kobilka, T. S., Thian, F. S., Edwards, P. C. *et al.* (2007). Crystal structure of the human  $\beta_2$  adrenergic G-protein-coupled receptor. *Nature*, **450**, 383–387.

6. Cherezov, V., Rosenbaum, D. M., Hanson, M. A., Rasmussen, S. G., Thian, F. S., Kobilka, T. S. *et al.* (2007). High-resolution crystal structure of an engineered human beta2-adrenergic G protein-coupled receptor. *Science*, **318**, 1258–1265.
7. Warne, T., Serrano-Vega, M. J., Baker, J. G., Moukhametzianov, R., Edwards, P. C., Henderson, R. *et al.* (2008). Structure of a  $\beta$ 1-adrenergic G-protein-coupled receptor. *Nature*, **454**, 486–491.
8. Jaakola, V. P., Griffith, M. T., Hanson, M. A., Cherezov, V., Chien, E. Y., Lane, J. R. *et al.* (2008). The 2.6 Ångstrom crystal structure of a human A<sub>2A</sub> adenosine receptor bound to an antagonist. *Science*, **322**, 1211–1217.
9. Murakami, M. & Kouyama, T. (2008). Crystal structure of squid rhodopsin. *Nature*, **453**, 363–367.
10. Wu, B., Chien, E. Y., Mol, C. D., Fenalti, G., Liu, W., Katritch, V. *et al.* (2010). Structures of the CXCR4 chemokine GPCR with small-molecule and cyclic peptide antagonists. *Science*, **330**, 1066–1071.
11. Kolb, P., Rosenbaum, D. M., Irwin, J. J., Fung, J. J., Kobilka, B. K. & Shoichet, B. K. (2009). Structure-based discovery of  $\beta$ 2-adrenergic receptor ligands. *Proc. Natl Acad. Sci. USA*, **106**, 6843–6848.
12. Sarkar, C. A., Dodevski, I., Kenig, M., Dudli, S., Mohr, A., Hermans, E. & Plückthun, A. (2008). Directed evolution of a G protein-coupled receptor for expression, stability, and binding selectivity. *Proc. Natl Acad. Sci. USA*, **105**, 14808–14813.
13. Grisshammer, R. & Tucker, J. (1997). Quantitative evaluation of neurotensin receptor purification by immobilized metal affinity chromatography. *Protein Expression Purif.* **11**, 53–60.
14. Chen, G., Hayhurst, A., Thomas, J. G., Harvey, B. R., Iverson, B. L. & Georgiou, G. (2001). Isolation of high-affinity ligand-binding proteins by periplasmic expression with cytometric screening (PECS). *Nat. Biotechnol.* **19**, 537–542.
15. Morishima, Y., Nakata, Y. & Segawa, T. (1989). Comparison of the effects of ions and GTP on substance P binding to membrane-bound and solubilized specific sites. *J. Neurochem.* **53**, 1428–1434.
16. von Heijne, G. & Gavel, Y. (1988). Topogenic signals in integral membrane proteins. *Eur. J. Biochem.* **174**, 671–678.
17. White, S. H. & von Heijne, G. (2004). The machinery of membrane protein assembly. *Curr. Opin. Struct. Biol.* **14**, 397–404.
18. Roth, C. B., Hanson, M. A. & Stevens, R. C. (2008). Stabilization of the human beta2-adrenergic receptor TM4-TM3-TM5 helix interface by mutagenesis of Glu122(3.41), a critical residue in GPCR structure. *J. Mol. Biol.* **376**, 1305–1319.
19. Angel, T. E., Chance, M. R. & Palczewski, K. (2009). Conserved waters mediate structural and functional activation of family A (rhodopsin-like) G protein-coupled receptors. *Proc. Natl Acad. Sci. USA*, **106**, 8555–8560.
20. Link, A. J., Skretas, G., Strauch, E. M., Chari, N. S. & Georgiou, G. (2008). Efficient production of membrane-integrated and detergent-soluble G protein-coupled receptors in *Escherichia coli*. *Protein Sci.* **17**, 1857–1863.
21. Skretas, G. & Georgiou, G. (2008). Engineering G protein-coupled receptor expression in bacteria. *Proc. Natl Acad. Sci. USA*, **105**, 14747–14748.
22. Massey-Gendel, E., Zhao, A., Boulting, G., Kim, H. Y., Balamotis, M. A., Seligman, L. M. *et al.* (2009). Genetic selection system for improving recombinant membrane protein expression in *E. coli*. *Protein Sci.* **18**, 372–383.
23. Standfuss, J., Xie, G., Edwards, P. C., Burghammer, M., Oprian, D. D. & Schertler, G. F. (2007). Crystal structure of a thermally stable rhodopsin mutant. *J. Mol. Biol.* **372**, 1179–1188.
24. Molina, D. M., Cornvik, T., Eshaghi, S., Haeggstrom, J. Z., Nordlund, P. & Sabet, M. I. (2008). Engineering membrane protein overproduction in *Escherichia coli*. *Protein Sci.* **17**, 673–680.
25. Zhou, Y. & Bowie, J. U. (2000). Building a thermostable membrane protein. *J. Biol. Chem.* **275**, 6975–6979.
26. Tate, C. G. & Schertler, G. F. (2009). Engineering G protein-coupled receptors to facilitate their structure determination. *Curr. Opin. Struct. Biol.* **19**, 386–395.
27. Li, B., Scarselli, M., Knudsen, C. D., Kim, S. K., Jacobson, K. A., McMillin, S. M. & Wess, J. (2007). Rapid identification of functionally critical amino acids in a G protein-coupled receptor. *Nat. Methods*, **4**, 169–174.
28. Beukers, M. W. & Ijzerman, A. P. (2005). Techniques: how to boost GPCR mutagenesis studies using yeast. *Trends Pharmacol. Sci.* **26**, 533–539.
29. Sommers, C. M. & Dumont, M. E. (1997). Genetic interactions among the transmembrane segments of the G protein coupled receptor encoded by the yeast STE2 gene. *J. Mol. Biol.* **266**, 559–575.
30. Tucker, J. & Grisshammer, R. (1996). Purification of a rat neurotensin receptor expressed in *Escherichia coli*. *Biochem. J.* **317**, 891–899.
31. Bennett, V. J. & Simmons, M. A. (2001). Analysis of fluorescently labeled substance P analogs: binding, imaging and receptor activation. *BMC Chem. Biol.* **1**, 1.